Journal of the Korean Magnetic Resonance Society **2001**, *5*, 110-117

^{19}F MR Imaging of 5-FU Metabolism in Mice

Seung-C. Lee[1], Jae-G. Seo[1], Sung W. Kim[2], Chulhyun Lee[1], Chul S. Kim[1], Taegyun Yang[1], and Chaejoon Cheong[1*]

[1]Magnetic Resonance Team, Korea Basic Science Institute, 52 Eoun-dong, Yusong-gu, Daejon 305-333, [2]Biomolecule Research Team, Korea Basic Science Institute, 52 Eoun-dong, Yusong-gu, Daejon 305-333

Received November 15, 2001

Abstract: ^{19}F imaging of mice was carried out. For ^{19}F imaging, 5-flouro-uracil (5-FU) was injected into a mouse and *in vivo* detection of the catabolism of 5-FU to α-fluoro-β-alanine (FBAL) was carried out. The chemical shift selective (CHESS) imaging technique was employed. The ^{19}F spectra and images give temporal and spatial information of the metabolism for 5-FU in mice.

INTRODUCTION

Magnetic resonance imaging (MRI) has been conventionally used as diagnostic imaging tools in hospitals. MRI technique can now be used for molecular imaging.[1-3] Molecular imaging is a research discipline aimed at developing novel tools and methods to image specific molecular pathways *in vivo*, particularly those that are key targets in disease processes. Among the often used such tools, e.g., PET, SPECT, and MRI, only MRI can distinguish different intermediates in metabolic pathways. 5-fluorouracil (5-FU) is an antineoplasmic drug and is catabolized to α-fluoro-β-alanine (FBAL) in animals.[4, 5] ^{19}F chemical shift selective (CHESS) imaging technique can give spatial and temporal information of the 5-FU and FBAL distribution in the body of animals, such as mice. The method is a kind of modalities for the detection of gene expression, since 5-FU is catabolized to FBAL only where an enzyme dihydropyrimidine dehydrogenase (DPD) is present. In normal mouse the enzyme is in its highest concentration in the liver. Another method to observe gene expression by MRI is using contrast agent which is activated when a specific gene is expressed. Louie *et al.* used this technique to observe gene expression in *Xenopus laevis* embryos by proton NMR.[6] Here, we report that the spatial distributions of 5-FU and FBAL have been separately imaged by ^{19}F CHESS technique.

*To whom : cheong@comp.kbsi.re.kr

MATERIALS AND METHODS

MR Technique

^{19}F imaging was carried out on a 9.4 T vertical bore microimaging system (Bruker, Germany). A double tuned $^{1}H/^{19}F$ multi-channel coil was used. The fluorine resonance frequency was 376.4 MHz and the proton resonance frequency was 400.1 MHz. Fig. 1 shows the CHESS imaging sequence employed for the chemical shift selective imaging. The first soft pulse of Gaussian shape was used for chemical shift selective spin excitation, and the second soft pulse of Sinc shape combined with the slice gradient was used for slice selective spin refocusing. A phantom sample was prepared to test the sequence. The phantom was composed of a 30 mm diameter tube containing another 10 mm diameter tube. Each cylinder contained 1 M TFA (Tri-fluoro acetic acid) solution and 0.1 M 5-FU solution, respectively. The two chemical shifts are separated by 95 ppm. The CHESS imaging sequence (Gaussian pulse bandwidth = 900 Hz, TH = 5 mm, FOV = 40 mm, MA = 64 × 64, TE = 7.3 ms, TR = 5000 ms, NEX = 1) was applied for each chemical shift.

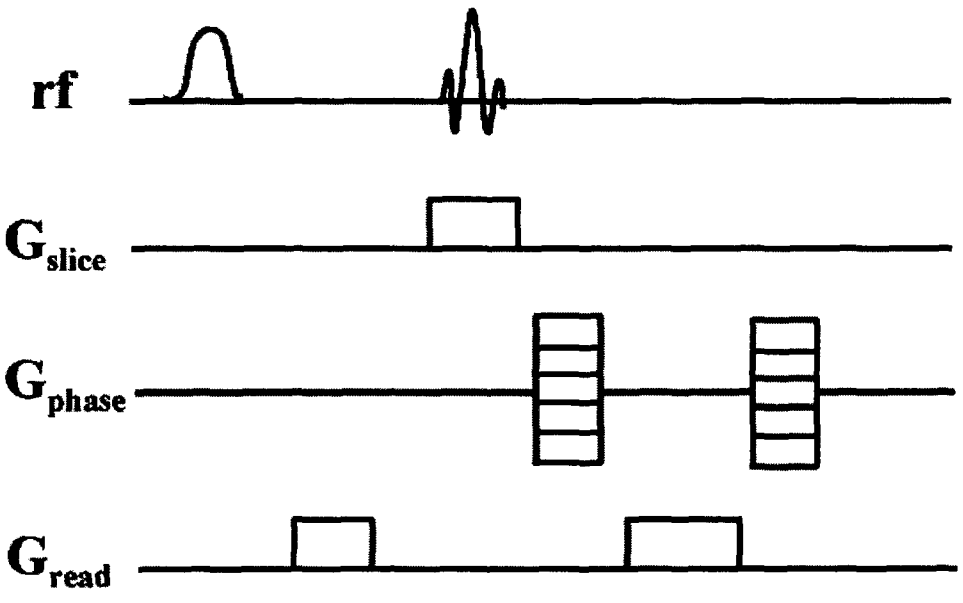

Fig.1 The pulse sequence of the chemical shift selective spin echo CHESS imaging. The first soft pulse of Gaussian shape is chemical shift selective, and the second pulse of Sinc shape is slice selective.

Animal study

Mice of 3 weeks from birth and of about 24 g body weights were chosen for our study. To accelerate the metabolic reaction of 5-FU in the liver, the mice were starved for 12 hours before 5-FU injection. 200 mg/kg body weight of 5-FU was injected to the tail vein of the mouse. The mice were kept in narcosis by intramuscular injection of an anaethetics, Avertin, 5 minutes before 5-FU injection. Avertin was prepared by mixing 10 g of tribromoethyl alcohol with 10 ml of tertiary amyl alcohol and was diluted to 2.5 %. T1 weighted multi-slice coronal ^{1}H spin echo images (TR = 600 ms, TE = 15 ms, NEX =1, MA = 256 ×128, TH = 1 mm, FOV = 40 mm) were acquired first to see the anatomical location of the mouse organs. ^{19}F NMR spectra (TR = 2000 ms, NEX =128) of the mouse were collected and the peaks from 5-FU and its catabolites were identified. ^{19}F chemical shift selective MR images (TR = 2000 ms, TE = 3.5 ms, FOV = 50 mm, MA = 32 × 16, TH = 40 mm, NEX = 64) were obtained with the center frequency at the 5-FU and FBAL peaks, respectively. Slice thickness was chosen so that it could cover the whole mouse body. The echo time was made as small as possible since the ^{19}F signal in the mouse body decreased fast with increasing echo time. For the purpose the chemical shift selective pulse and refocusing pulse of only 1 ms duration were employed. While shortening pulse length brought enlargement of chemical shift selection bandwidth, there was no problem in getting chemical shift selective images in our purpose owing to the large chemical shift difference between 5-FU and FBAL. The matrix size was chosen small to get high SNR from the weak fluorine signal. Linear smoothing and low pass filtering have been applied in image processing.

RESULTS AND DISCUSSION

Fig. 2 shows the phantom CHESS images selective for TFA (a) and 5-FU (b). The two regions are sharply discriminated. The dark part around the tube edge in Fig. 2(a) comes from the inhomogeneity of the RF coil. Figure 3(a) is the ^{19}F spectrum of a 5-FU injected mouse, taken 10 minutes after the injection. A dominant 5-FU peak is seen and referenced as 0 ppm, and at around -18 ppm the minor peaks of the 5-FU catabolites are also seen. Figure 3(b) is a coronal slice proton image of the mouse, which shows the anatomical location. Figure 3(c) is the 5-FU image collected for 30 minutes beginning at 20 min. after 5-FU injection. Figure 3(c) shows the distribution of the drug 5-FU in the mouse body at the early time after 5-FU injection. The drug is distributed at most of the internal organs and at the brain. Figure 4 shows images of 5-FU and FBAL distribution in the mouse body. Figure 4(a) shows the proton image and Fig. 4(b) shows the 5-FU image taken 40 minutes after 5-FU injection. Figure 4(c) is the FBAL image whose data collection started 1 hr after 5-FU injection. The image shows that FBAL is detected in the liver and the bladder. It means that at this time the catabolic reaction to FBAL has occurred in the liver and some FBAL has been delivered to the bladder. Figure 4(d) is another FBAL image taken 1hr 35 minutes after

the initial 5-FU injection. At this time most FBAL has been transported to the bladder. Compared to the 5-FU distribution in Fig. 3, 5-FU is now seen only in the bladder. It means that some 5-FU has been transported directly to the bladder. Figures 5(a), 5(b) and 5(c) are the ^{19}F spectra measured at 20 min., 40 min., and 2 hr. after the 5-FU injection to the mouse. The successive spectra show the increase of the final catabolite FBAL. The peak at -18.8 ppm is the FBAL peak, and the peak at –17.2 ppm is that of α-fluoro-β-ureidopropionate which is the second catabolite of 5-FU.[7] The first catabolite of 5-FU, dihydro-5-fluorouracil, is not seen. It means that the processes from the first product to the second and to the third products are very rapid, while the process from 5-FU to the first product is relatively slow. It is consistent with the previous report that the first catabolism process, which is governed by the enzyme, DPD, is the rate limiting step for the whole process from 5-FU to FBAL.[7] Another observation from Fig. 5 is that the linewidths of the peaks in Fig. 5(a) are broader than those in Fig. 5(c). It implies that 5-FU and FBAL in Fig. 5(a) are from tissues and those in Fig. 5(c) are from urine in the bladder. It is consistent with the obtained ^{19}F images. In Fig. 5(b), the linewidth of 5-FU is already very sharp, which means that 5-FU has moved to the bladder already at this time.

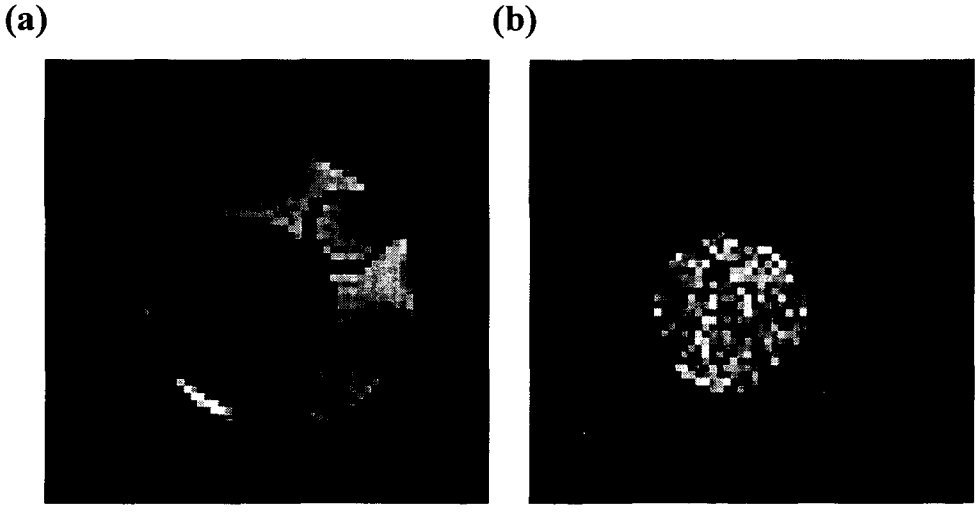

Fig.2 (a) The phantom image from CHESS imaging of TFA peak. The inner black disk is the region filled with 5-FU. The image shows another small disk filled with TFA solution. **(b)** The phantom image from CHESS imaging of 5-FU peak. The difference between the disk diameters of (a) and (b) comes from the inner tube thickness. The SNR difference between the two images comes from the difference in ^{19}F concentration.

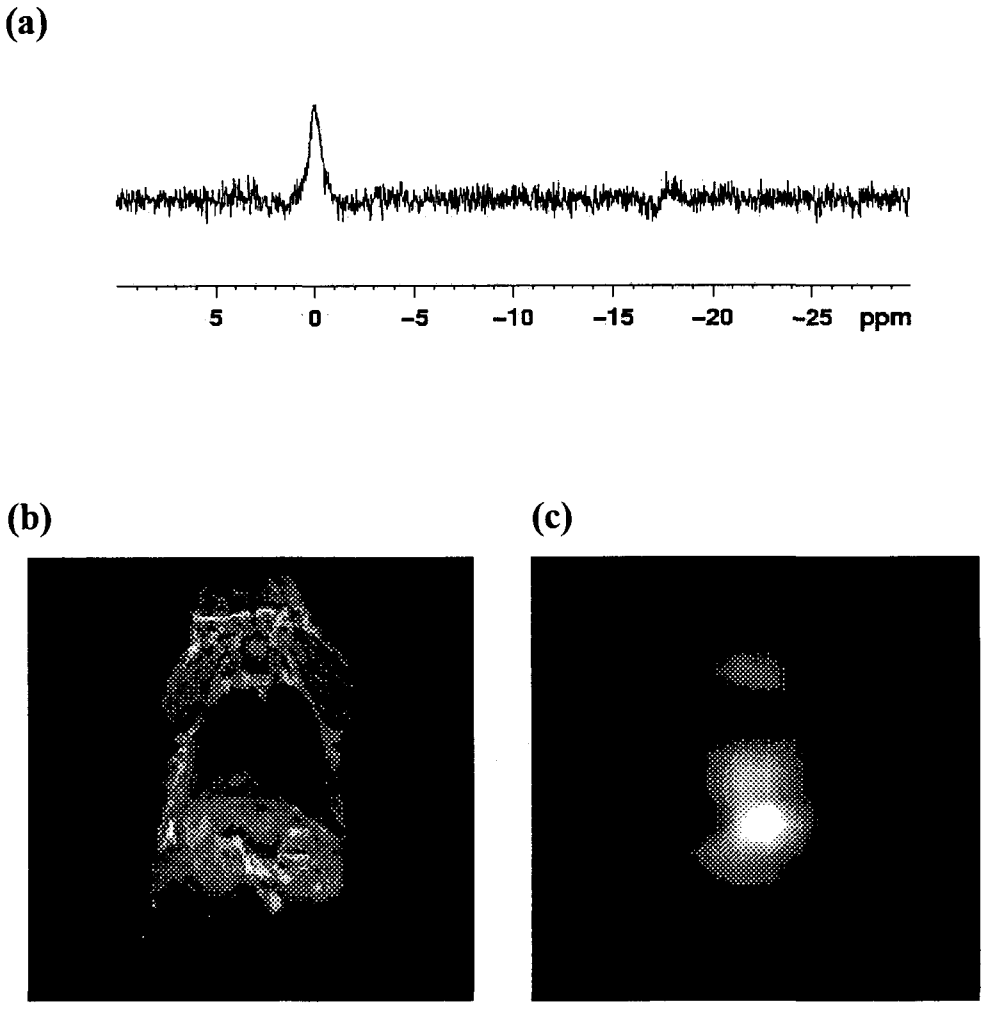

Fig.3 (a) The ^{19}F spectrum of a 5-FU injected mouse taken 10 min. after 5-FU injection. The dominant 5-FU peak and the peaks from catabolites around -18 ppm are shown. **(b)** A coronal slice proton image of the mouse **(c)** The CHESS 5-FU image of the mouse collected for 30 minutes beginning at 20 min. after 5-FU injection. The 5-FU is distributed at most internal organs and at the brain.

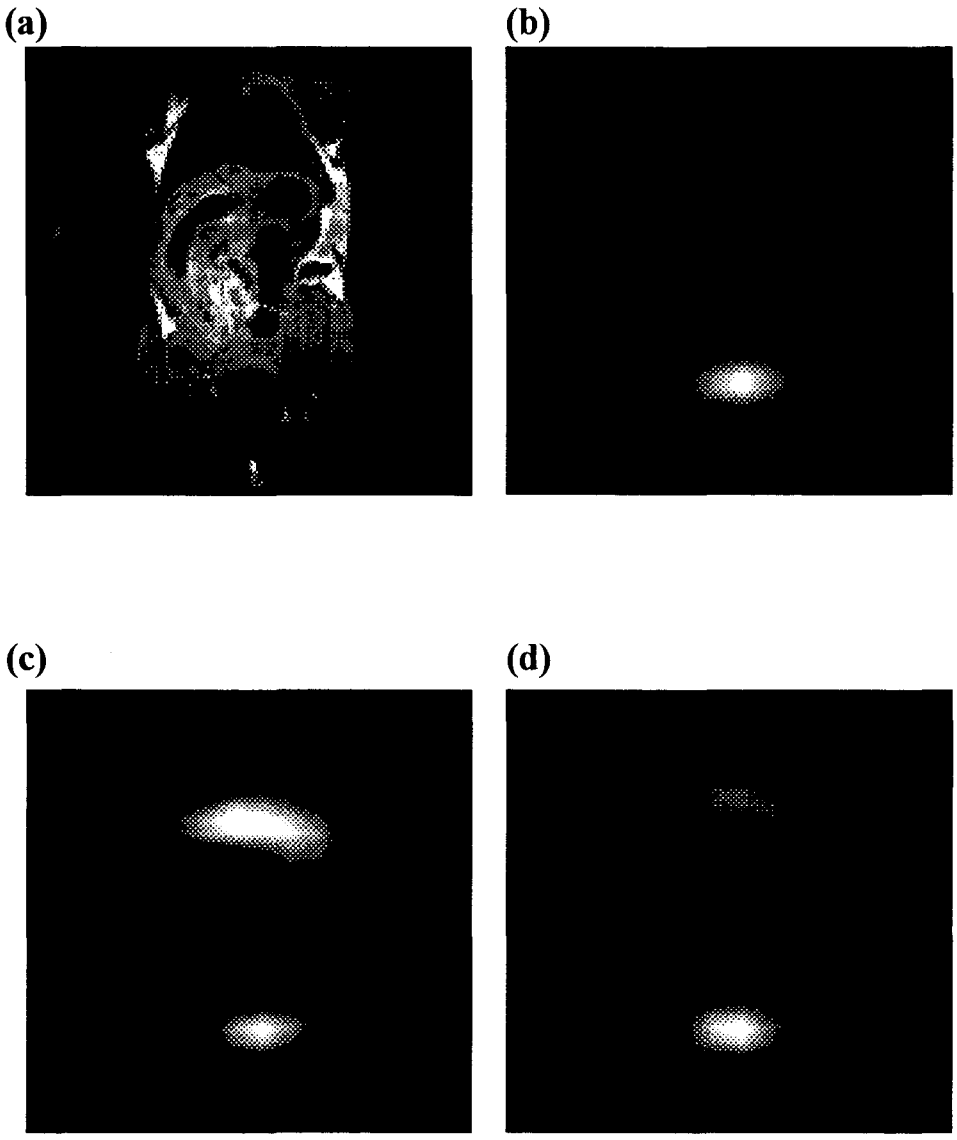

Fig.4 **(a)** A coronal slice proton image of the mouse **(b)** The CHESS 5-FU image of the mouse taken 40 min. after 5-FU injection. **(c)** The CHESS FBAL image of the mouse taken 1 hr. after 5-FU injection **(d)** The CHESS FBAL image of the mouse taken 1 hr. 35 min. after 5-FU injection

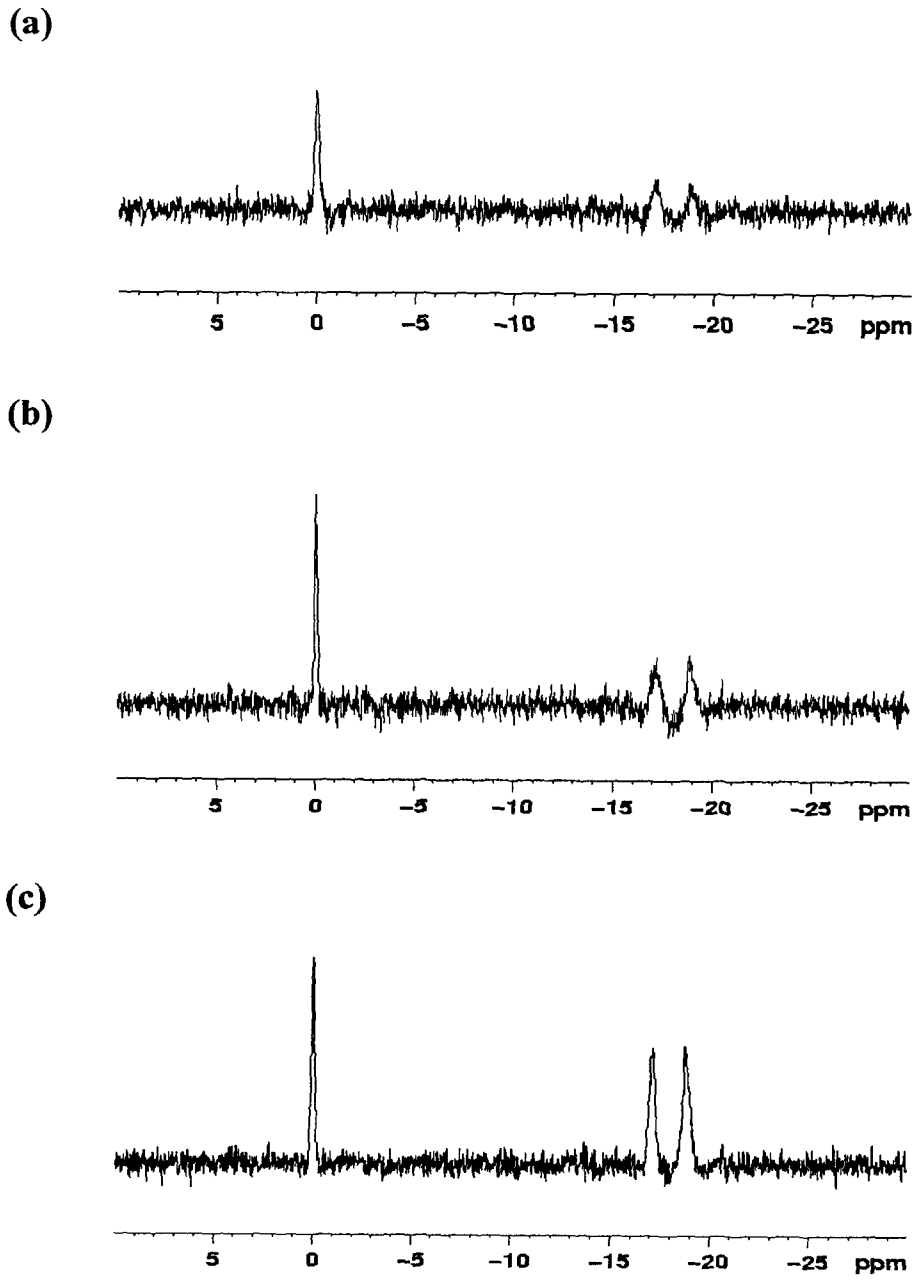

Fig. 5 The ^{19}F spectra of the mouse measured at **(a)** 20 min. **(b)** 40 min., and **(c)** 2 hr. after 5-FU injection.

CONCLUSION

In this research we observed the temporal and spatial distributions of 5-FU and FBAL when 5-FU was injected to mice. The results are significant since by this technique we can trace metabolic changes in the body of live animals. The results also indicate that detection gene expression whose function is of interest is possible. In our case, it has been shown that DPD resides mostly in liver.

Acknowledgment
This work was financially supported by the Ministry of Science and Technology (Grant 00-J-LF-01-B-41).

REFERENCES

1. J. D. Bell and S. D. Taylor-Robinson, *Gene Therapy* **7,** 12159 (2000)
2. R. Weissleder and U. Mahmood, *Radiology* **219 (2),** 316 (2001)
3. D. Wagenarr, R. Weissleder, A. Hengerer, *Academic Radiology* **8 (5),** 409 (2001)
4. G. Brix, M. E. Bellemann, H.-J. Zabel, P. Bachert, and W. J. Lorenz, *Mag. Res. Imag.* 1193 (1993)
5. G. Brix, M. E. Bellemann, U. Haberkorn, L. Gerlach, P. Bachert, and W. J. Lorenz, *Mag. Reson. Med.* **34,** 302 (1995)
6. A. Y. Louie, M. M. Huber, E. T. Ahrens, U. Rothbacher, R. Moats, R. E. Jacobs, S. E. Fraser, and T. J. Meade, *Nature* **18,** 321 (2000)
7. F. N. M. Naguib et al., *Cancer Research* **45,** 5405 (1985)